Available online at www.sciencedirect.com
ScienceDirect
Mendeleev Commun., 2020, **30**, 772–774
Mendeleev Communications

Electrolytic PdMo deposits with high corrosion resistance in relation to palladium

Vitaly V. Kuznetsov,*[a,b] Alina V. Telezhkina[a] and Boris I. Podlovchenko[c]

[a] *D. I. Mendeleev University of Chemical Technology of Russia, 125047 Moscow, Russian Federation. Fax: +7 499 978 8660; e-mail: vitkuzn1@mail.ru*
[b] *National Research Nuclear University MEPhI, 115409 Moscow, Russian Federation*
[c] *Department of Chemistry, M. V. Lomonosov Moscow State University, 119991 Moscow, Russian Federation. Fax: +7 495 939 0171; e-mail: podlov@elch.chem.msu.ru*

DOI: 10.1016/j.mencom.2020.11.028

The PdMo (~20 at% Mo) deposits obtained by electrodeposition from acetate solutions containing a palladium salt and ammonium heptamolybdate on the surface of a glassy carbon electrode demonstrated low palladium solubility at high anodic potentials.

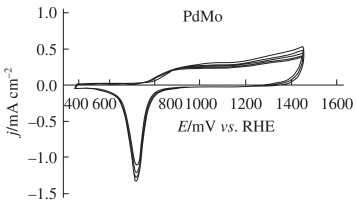

Keywords: electrodeposition, palladium–molybdenum alloy, corrosion, corrosion resistance, palladium, molybdenum, surface oxides, anodic potentials.

Nanostructured PdMo alloys are promising electrocatalysts for the reduction of oxygen and the oxidation of small organic molecules under conditions of low-temperature fuel cells.[1–3] Like other palladium-containing catalysts, the PdMo catalysts are characterized by relatively low corrosion resistance of Pd.[2,4] The influence of non-noble metal additives on the electrochemical dissolution of palladium is poorly known.[5–7] Mixed electrolytic deposits (e.d.) are convenient model systems for studying catalytic activity and corrosion resistance of Pd–M composites.[7–9] An important requirement for such deposits is relatively small changes in their composition and state during corrosion tests. On the other hand, the concentration of metals in a corrosive solution should be sufficient for measurements by analytical methods. The aim of this study was to reveal the impact of molybdenum on the electrochemical dissolution of palladium using an example of mixed e.d. PdMo. Since the electrochemical deposition of molybdenum from aqueous solutions is hindered,[10] obtaining mixed PdMo electrodeposits meeting the requirements of quantitative corrosion studies was a separate task.

Electrodeposition was carried out in a three-electrode cell in a solution stirred by a stream of argon. An attempt to obtain PdMo electrodeposits on a glassy carbon electrodes from citric solutions containing sodium molybdate and palladium chloride by analogy with a published procedure[11] was undertaken initially. The solutions of 0.2 M Na_3Cit + 0.04 M Na_2MoO_4 + 0.1 M KCl + + x M $PdCl_2$ ($x = 0.04$–0.08) were used. Only thin films containing no more than 12 at% Mo were synthesized in these experiments. They were not suitable for a correct study of the effect of Mo additives on the electrochemical corrosion behavior of dispersed palladium.

As found previously,[10,12,13] the electroreduction of Mo^{VI} species to a metallic state from ammonium acetate solutions can occur at high cathode potentials. Based on these results, the solutions containing 4 M KAc + 4 M NH_4Ac + 0.035 M $(NH_4)_6Mo_7O_{24}$ + x M $PdCl_2$ ($x = 0.001 - 0.005$ M) at pH 9.0 ± 0.2 were chosen for the electrodeposition of PdMo alloys. Glassy carbon (GC) electrodes with $S_{geom} = 1$ cm^2 were used as substrates. Electrodeposition of PdMo coatings was carried out in the galvanostatic mode at j = 0.125–0.75 A cm^{-2} for 10 min. The effect of Mo additives on the electrochemical behavior of Pd was tested by comparing the characteristics of e.d. PdMo with those of e.d. Pd obtained under the same conditions in a similar solution, which did not contain ammonium heptamolybdate. The electrolytic deposits were characterized.[†]

The electrochemical corrosion of PdMo alloys in the anodic potential region was studied under potentiodynamic conditions with a linear potential sweep (ν = 2 mV s^{-1}) in a 0.5 M aqueous solution of H_2SO_4. The experiments were performed in a three-electrode cell with separated cathode and anode compartments under an argon atmosphere at 20 ± 2 °C. A reversible hydrogen electrode (RHE) in the same solution was used as a reference electrode. The working electrode compartment volume of the electrochemical cell was 50 cm^3. The electrode potential was scanned within a region of 0.45–1.45 V (hereinafter, all potentials are given *vs*. RHE).

[†] The bulk chemical composition of the coatings was determined by X-ray microanalysis using a Hitachi TM–3000 scanning electron microscope (Japan) equipped with a Link microprobe analyzer (Oxford). The composition of the deposits was determined at no less than 10 points on the surface. The spot diameter was ~0.6 μm, and the analytical depth was ~1 μm. After that, the data were statistically processed. A comparison of the X-ray microanalysis data with the results of AES ICP analysis performed after the dissolution of e.d. in nitric acid showed a good agreement (±5%). The phase composition of the coatings was analyzed using a Philips PW1820/00 diffractometer with CuKα radiation (λ = 0.15406 nm). The chemical composition of the surface layers and the oxidation degrees of the elements in them were determined by X-ray photoelectron spectroscopy (XPS) on an HB100 spectrometer (Vacuum Generators, GB) using AlKα radiation (radiation energy, 1486.6 eV; power, 200 W).

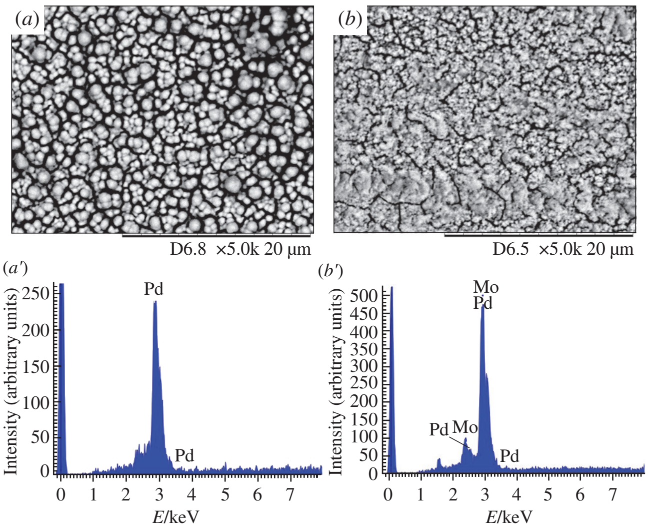

Figure 1 (*a*, *b*) Morphology and (*a*′, *b*′) EDX spectra of (*a*, *a*′) electrodeposited Pd and (*b*, *b*′) PdMo obtained from an ammonium acetate solution.

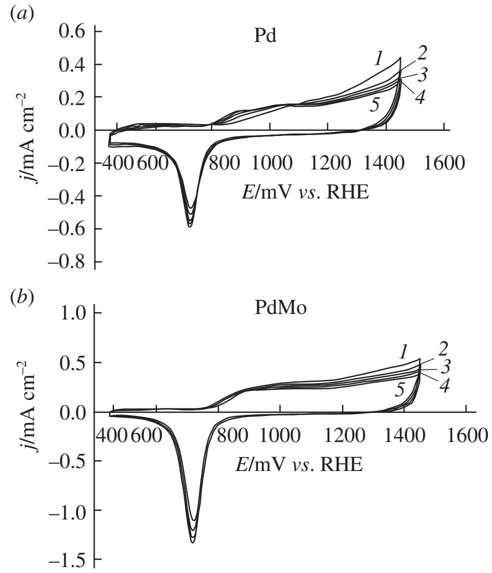

Figure 2 Cyclic voltammograms of (*a*) electrodeposited Pd/GC and (*b*) PdMo/GC electrodes in 0.5 M H_2SO_4. Scanning potential rate $v = 2$ mV s^{-1}. The cycle numbers are indicated.

Three polarization modes were used, namely: I, full cyclic voltammograms (CVA) in the indicated region of electrode potentials; II, the sweep of potential from 0.45 to 1.45 V followed by a potential jump to 0.45 V; and III, four anodic sweeps of the electrode potential in a range of 0.45–1.45 V with a potential jump to 0.45 V after II. The electrode potential semi-cycles in modes II and III were applied to minimize both solution redeposition and the restructuring of electrode deposits during a slow cathode potential sweep.[7,14] Programs I and II were performed with freshly deposited metals. The chemical analysis of the solution after polarization modes I–III was carried out by ICP-AES. For this purpose, a solution sample (1 cm^3) was taken from the working compartment of the electrochemical cell.

Pd and Mo were detected in PdMo electrodeposits by EDX analysis [Figure 1(*b*′)]. Non-metallic impurities were not found. Atomic percentages of Pd and Mo depend on the cathodic current density used for electrodeposition of alloy (Table 1). Obviously, changes in the values of Δm and δ in the range $j = 0.125$–0.5 A cm^{-2} are within the limits of experimental error.

Electrode deposits containing 18 ± 2 at% molybdenum obtained at a current density of 0.25 A cm^{-2} were chosen for further studies. According to SEM data, both PdMo and Pd deposits had large surface areas.

The rather high dispersion of the freshly obtained deposits is indicated by a large peak at the cathodic scan of CVAs that corresponds to the reduction of O_{ads} [Figures 2(*a*) and 2(*b*), curves *1*]. Since the upper limit of potential scanning was 1.45 V *vs*. RHE, oxygen was adsorbed on the Pd surface in an amount much larger than that for the monolayer. This makes it difficult to exactly determine the true surface of Pd (S_{true}).[14,15] However, the ratio of areas on O_{ads} desorption peaks on cathodic scans of PdMo and Pd electrodeposits obviously can be used for a rough estimation of changes in the dispersity of Pd deposits due to the inclusion of Mo. Such a comparison gives the value of $S_{true}(PdMo)/S_{true}(Pd) = \sim 2.5$ for freshly deposited coatings (Figure 2) to indicate an increase in the dispersity of deposits. A similar effect was observed when lead or copper was included in palladium electrodeposits.[7,14] Cyclic voltammograms (CVs) of PdMo electrodeposits in 0.5 M H_2SO_4 were stable in the course of potential scanning up to 1.45 V (Figure 2). An increase in the number of cycles did not significantly change both the shape of voltammograms and the charge corresponding to O_{ads} desorption to demonstrate the unusual stability of e.d. PdMo in the anode region of potentials. This can be due to the formation of a mixed oxide film of $PdMoO_x$ at the electrode surface under conditions of anodic polarization. Such a process occurred in mixed $Pd^0(Cu)$ deposits.[16] A difference in the adsorption of oxygen at Pt and PtMo electrodeposits caused different changes in the shape of anodic scans of cyclic voltammograms during multiple scanning electrode potential [Figures 2(*a*),(*b*)] at the potentials corresponding to the onset of oxygen adsorption (0.8–1.0 V).

Table 1 Properties of electrochemical PdMo deposits obtained from acetate solution as a function of cathode current density.

Current density, j/A cm^{-2}	x(Pd)/ at%	x(Mo)/ at%	Deposit weight Δm^a/mg cm^{-2}	Average deposit thickness δ^b/μm
0.125	69 ± 2	31 ± 2	0.6	0.5
0.25	82 ± 2	18 ± 2	0.6	0.5
0.50	81 ± 2	19 ± 2	0.6	0.5
0.75	78 ± 2	22 ± 2	1.0	0.8

^{a}Measured using an analytical microbalance. ^{b}Calculated under the assumption of a uniform coating thickness.

Relatively large anodic currents on the first scan of the cyclic voltammograms at $E > 1.2$ V correspond to the processes of molybdenum and palladium dissolution, adsorption of oxygen atoms on Pd, and transitions of molybdenum oxides from low oxidation states to higher ones. Note that the currents of molybdenum dissolution for PdMo electrodeposits are significantly lower compared to metallic molybdenum. The vigorous dissolution of molybdenum associated with passive film breakdown occurs at potentials more positive than ~0.4 V.[17,18] It could be assumed that the palladium matrix hindered the dissolution of molybdenum. This assumption was supported by the fact that reflexes corresponding to molybdenum-containing phases were absent from the diffractograms (Online Supplementary Materials). A broad diffuse maximum at $2\theta \approx 40°$ is likely associated with the Pd(111) reflex broadened due to small sizes of palladium clusters. Apparently, the Pd–Mo electrochemical deposits obtained from acetic solutions are solid solutions of molybdenum in palladium. According to a phase diagram,[19] molybdenum is soluble in palladium. In this case, the oxidized states of molybdenum are present only in a thin surface layer.

High-resolution XPS spectra showed that palladium at the surface of PdMo electrodes is primarily in a metallic state before the corrosion test [Figure 3(*b*)]. Molybdenum is basically in

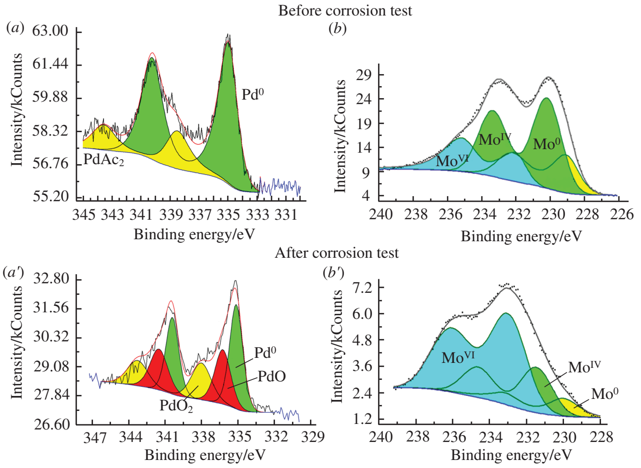

Figure 3 High resolution (*a*, *a*′) Pd 3*d* and (*b*, *b*′) Mo 3*d* XPS spectra (*a*, *b*) before and (*a*′, *b*′) after the corrosion test.

oxidized states. The XPS peaks correspond to Mo^{VI}, Mo^{IV}, and Mo^0. The oxidation of both palladium and molybdenum in the surface layers occurs during potential scanning. This follows from the XPS spectra recorded at the surface of PdMo electrodes after the corrosion test. Pd^{II} and even Pd^{IV} species appear in the surface layers of the electrode after potential scanning (see Figure 3). The fraction of oxidized states of Mo is also increasing. In general, this is consistent with the above assumptions on the nature of changes in the surface layer based on voltammetric measurements.

The weights of palladium dissolved in the course of potential scanning are given in Table 2 for Pd [*m*(Pd)] and PdMo [*m*(PdMo)] electrodeposits.

The experimental data revealed that the average rate of palladium dissolution from PdMo alloy decreased by a factor of 5–10, as compared to Pd deposits. Molybdenum species formed in the surface layers of PdMo deposits inhibit the dissolution of palladium. The dissolution of molybdenum is significant; however, Mo was detected in the surface layers of PdMo electrodes after five polarization cycles (see Figure 3). Its amount slightly increased after the anodic dissolution of the alloy. The ratio of palladium and molybdenum atomic fractions x(Mo)/x(Pd) changed from 0.23 before potential cycling to 0.31 after cycling (polarization mode III). The atomic ratio of the amounts of dissolved Mo to dissolved Pd was several times greater than 1 (see Table 2), which suggests that the mechanism of anodic dissolution of the PdMo deposits differs from that assumed for e.d. PdPb and PdCu.[7,14]

A significant increase in the rate of solubility of Pd deposits when copper or lead was included in their composition was observed previously.[7,14] This was due to an increase in the dispersity of e.d. Comparing these data with the above results for e.d. PdMo, we can note an unusual inverse effect, namely, an increase in the corrosion resistance of Pd when a small amount of non-noble metal was added to it. This effect occurred despite an increase in the dispersity of electrolytic deposits. Cubic crystal structures of molybdenum and palladium and a slightly smaller atomic radius of Mo (0.136 nm), compared to that of Pd (0.138 nm), should facilitate the formation of the alloys of these metals with high corrosion resistance.[14,20] However, it is likely that the major cause for such a high corrosion resistance of PdMo deposits compared to Pd deposits is the presence of various Mo oxides in their surface layers, *i.e.*, the high oxophilicity of Mo. It can be assumed that the electrodissolution of palladium in the test region of potentials (up to 1.45 V) mainly proceeds through the direct reaction Pd → Pd^{2+} + 2e (ref. 21) rather than palladium oxides. The presence of Mo oxides can significantly reduce the fraction of the surface occupied by unoxidized palladium and, therefore, decrease the rate of its electrodissolution. An increase in the oxidation state of Pd in the surface layers of the electrode was indicated by XPS data.

Table 2 Results on the dissolution of palladium and molybdenum during the anodic polarization of e.d. Pd and e.d. PdMo in 0.5 M H_2SO_4.

Sample	Mode	*m*(Pd)/μg	*m*(PdMo)/*m*(Pd)	*m*(Mo)/μg	at. Mo/at. Pd
e.d Pd	I	21	0.12		
	II	12	0.16		
	III	22	0.21		
e.d PdMo	I	2.5		15.0	6.0
	II	2.0		7.0	3.5
	III	4.5		13.5	3.0

This work was supported by the Russian Foundation for Basic Research (project no. 19-03-00309) and, in part, by M. V. Lomonosov Moscow State University Program of Development.

Online Supplementary Materials

Supplementary data associated with this article can be found in the online version at doi: 10.1016/j.mencom.2020.11.028.

References

1 M. Luo, Z. Zhao, Y. Zhang, Y. Sun, Y. Xing, F. Lv, Y. Yang, X. Zhang, S. Hwang, Y. Qin, J.-Y. Ma, F. Lin, D. Su, G. Lu and S. Guo, *Nature*, 2019, **574**, 81.
2 H. Meng, D. Zeng and F. Xie, *Catalysts*, 2015, **5**, 1221.
3 V. V. Kuznetsov, K. V. Kavyrshina and B. I. Podlovchenko, *Mendeleev Commun.*, 2012, **22**, 206.
4 D. A. J. Rand and R. Woods, *J. Electroanal. Chem.*, 1972, **35**, 209.
5 M. R. Tarasevich, V. A. Bogdanovskaya, L. N. Kuznetsova, A. D. Modestov, B. N. Efremov, A. E. Chalykh, Yu. G. Chirkov, N. A. Kapustina and M. R. Ehrenburg, *J. Appl. Electrochem.*, 2007, **37**, 1503.
6 B. I. Podlovchenko, Yu. M. Maksimov, K. I. Maslakov, D. S. Volkov and S. A. Evlashin, *J. Electroanal. Chem.*, 2017, **788**, 217.
7 B. I. Podlovchenko, Yu. M. Maksimov, D. S. Volkov and S. A. Evlashin, *J. Electroanal. Chem.*, 2020, **858**, Article 113787.
8 M. Łukaszewski and A. Czerwiński, *J. Electroanal. Chem.*, 2006, **589**, 87.
9 B. I. Podlovchenko, Yu. M. Maksimov and D. O. Shkil, *Mendeleev Commun.*, 2019, **29**, 312.
10 T. J. Morley, L. Penner, P. Schaffer, T. J. Ruth, F. Bénard and E. Asselin, *Electrochem. Commun.*, 2012, **15**, 78.
11 D. D. Demir, A. Salcı and R. Solmaz, *Int. J. Hydrogen Energy*, 2018, **43**, 10530.
12 R. Syed, S. K. Ghosh, P. U. Sastry, G. Sharma, R. C. Hubli and J. K. Chakravartty, *Surf. Coat. Technol.*, 2015, **261**, 15.
13 V. V. Kuznetsov, M. A. Volkov, D. A. Zhiruhin and E. A. Filatova, *Russ. J. Electrochem.*, 2018, **54**, 1006 (*Elektrokhimiya*, 2018, **54**, 1025).
14 B. I. Podlovchenko, T. D. Gladysheva, Yu. M. Maksimov, D. S. Volkov and K. I. Maslakov, *J. Solid State Electrochem.*, 2020, **24**, 1439.
15 M. W. Breiter, *J. Electroanal. Chem.*, 1977, **81**, 275.
16 B. I. Podlovchenko, T. D. Gladysheva, Yu. M. Maksimov, K. I. Maslakov and D. S. Volkov, *J. Electroanal. Chem.*, 2019, **840**, 376.
17 A. A. Pozdeeva, E. I. Antonovskaya and A. M. Sukhotin, *Corr. Sci.*, 1966, **6**, 149.
18 V. V. Kuznetsov, K. V. Kavyrshina and B. I. Podlovchenko, *Russ. J. Electrochem.*, 2012, **48**, 467 (*Elektrokhimiya*, 2012, **48**, 513).
19 *Diagrammy sostoyaniya dvoinykh metallicheskikh system* (*Phase Diagrams for Two-Component Metal Systems. Handbook*), ed. N. P. Lyakishev, Mashinostroenie, Moscow, 1996, vol. 3 (in Russian).
20 K. Jiang, H.-X. Zhan, S. Zou and W.-B. Cai, *Phys. Chem. Chem. Phys.*, 2014, **16**, 20360.
21 E. Pizzutilo, S. Geiger, S. J. Freakley, A. Mingers, S. Cherevko, G. J. Hutchings and K. J. J. Mayrhofer, *Electrochim. Acta*, 2017, **229**, 467.

Received: 27th July 2020; Com. 20/6274